Study of the Electroconductive Properties of Conductive Polymers-Graphene/Graphene Oxide Nanocomposites Synthesized via *in Situ* Emulsion Polymerization

Syed Muhammad Imran,[1,2] Ali Salman,[3] Godlisten N Shao,[1,4] M Salman Haider,[1,5] Nadir Abbas,[1] SungSoo Park,[1] Manwar Hussain,[1] Hee Taik Kim[1]

[1]*Department of Fusion Chemical Engineering College of Engineering Sciences, Hanyang University, Ansan, Gyeonggi 426-791, Republic of Korea*

[2]*Department of Chemical Engineering, COMSATS Institute of Information Technology, Lahore, Pakistan*

[3]*School of Chemical and Materials Engineering, National University of Science and Technology (NUST), Islamabad, Pakistan*

[4]*Department of Chemistry, Mkwawa College, University of Dar Es Salaam, Iringa, United Republic of Tanzania*

[5]*Department of Chemical Engineering, University of Gujrat, HH Campus, Punjab, Pakistan*

The present study introduces a modified approach to synthesize polyaniline (PANI) and polypyrrole (PPy) doped with graphene oxide (GO) or graphene (GN) through an *in situ* emulsion polymerization (EP) technique. Dodecyl benzene sulfonic acid (DBSA) was used as a surfactant and doping agent as well during the polymerization reaction. The morphology and microstructure of the synthesized polymers and their nanocomposites were studied by scanning electron microscopy, transmission electron microscopy, Fourier transform infrared spectroscopy, X-ray photoelectron spectroscopy, and thermogravimetric analysis. All of these characterization techniques confirmed the superior morphology and thermal properties of the nanocomposites. The electroconductive properties of the synthesized polymers and their nanocomposite pellets containing 5 wt% of either GN or GO pressed at pressures of 2, 4, and 6 tons were investigated with a four-probe analyzer. Nanocomposites showed very high electrical conductivity compared to individual PANI and PPy samples pressed at the same pressures. The addition of GO and GN not only improved the thermal stability but also significantly enhanced the electrical conductivity of the nanocomposites. Thus, the present work signifies the importance of the direct loading of GO and GN into conductive polymers during the EP process using DBSA as a surfactant to achieve nanocomposites with promising properties for various semiconductive applications. POLYM. COMPOS., 39:2142–2150, 2018. **© 2016 Society of Plastics Engineers**

INTRODUCTION

Novel carbon-based structures, such as carbon nanotubes (CNTs), graphene (GN), and graphene oxide (GO), have attracted much attention in recent years for a variety of new technological applications [1]. Due to their excellent conductivity and large surface area, carbon materials are considered to be an ideal candidate for various electronic applications. Compared to CNTs, GN- and GO-based materials show many advantages such as their ability to be mass-produced at low cost, their large surface area, and their superior mechanical and electrical properties. GN sheets consist of two-dimensional, all-sp2-hybridized carbons and GO consists of 2D networks of

This article was published online on 09 August 2016. An error was subsequently identified. This notice is included in the online and print versions to indicate that both have been corrected 18 August 2016.

Correspondence to: H.T. Kim; e-mail: khtaik@yahoo.com and khtaik@hanyang.ac.kr or M. Hussain; e-mail: manwarh@hanyang.ac.kr

Contract grant sponsor: Korea Institute of Energy Technology Evaluation and Planning (KETEP) of the Ministry of Trade, Industry and Energy of the Republic of Korea; contract grant number: 20154030200680.

DOI 10.1002/pc.24179

Published online in Wiley Online Library (wileyonlinelibrary.com).

© 2016 Society of Plastics Engineers

sp2- and sp3-bonded atoms. These are regarded as ideal candidates for thin film materials and can also be used as electron accepting materials in organic solar cells due to their unique structural, electrochemical, and electronic properties [2–4].

Meanwhile, conducting polymer nanocomposites are attractive for many applications because of their low weight, low-cost corrosion resistance, ease of processing, and unique morphology/structure, which influence their physical and electrochemical properties. They are a class of polymeric materials with conjugated unsaturated bonds at the main chains. Combinations of these polymers with various carbon materials facilitate the formation of nanocomposites that are suitable for different electrical and electronic applications. To date, different functional nanocomposites with the combinations of polyaniline (PANI) and polypyrrole (PPy) with GO/GN have been extensively studied in attempts to produce materials with specific electrochemical, thermal, and mechanical properties [3, 5–8]. The obtained nanocomposites have been widely applied as solid state electrodes for batteries, electrolyte capacitors, shielding materials, corrosion protection, light-emitting diodes, solar cells, and chemical sensors [9].

Generally, PANI and PPy can be synthesized through chemical polymerization of their respective monomers in aqueous acidic media in the presence of an oxidant [10]. The final product obtained with this approach is usually irregular, in powder form, and often has a low degree of crystallinity and molecular orientation. This lowers the electrical conductivity and limits the applications of these polymers [11]. The conductivity of conductive polymers mainly depends on their ability to transport charge carriers along the polymer backbone and for the carriers to hop between polymer chains. Zhang [12] and Xia et al. [13] found that the conductivity of conductive polymers is the sum of the interchain and intrachain conductivities. In the case of coil-like conformations, the intrachain conductivity increases, while high polymer crystallinity results in an increase in the interchain conductivity. PPy can be prepared by electrochemical polymerization or chemical oxidative polymerization of the pyrrole monomer. The harsh conditions used during the polymerization of these conductive polymers can also decrease the electrical conductivities and reduce the overall electrochemical properties of the resulting polymers, which suggests that polymers with good electrochemical properties should be synthesized under milder conditions [9, 14]. Various researchers have reported [14–17] that the electrochemical and thermal properties of conductive polymers, including PANI and PPy, are greatly influenced by the polymerization conditions and the types of dopants that are used during polymerization.

Surfactants play an important role during the synthesis of conductive polymers. They are used to improve the properties of the resulting polymers in term of their stability, solubility in different organic solvents, and to enhance their electrical and thermal conductivities by acting as a dopant during the polymerization; thus, they can become a part of the resulting material [18, 19]. It has been further suggested that the presence of surfactants can improve the colloidal solubility and processability of conductive polymers in different organic solvents and that surfactant micelles control the distribution of reactants between the aqueous phase and micelles, which can alter the locus and path of polymerization. It has also been reported that the presence of surfactants during the polymerization of PANI and PPy leads to an increase in their conductivity [14, 17, 20–23].

Our research group has carried out different studies in attempts to fabricate nanocomposites of various conductive polymers doped with GO and GN [9, 17]. In our work, we have determined that samples with 5 wt% GO and GN show high electrical and thermal properties. Therefore, the present study compares the electrical properties of PANI and PPy nanocomposites with 5 wt% of GN and GO synthesized using a simple and reproducible *in situ* emulsion polymerization (EP) route. The polymerization process was carried out in the presence of a functionalized protonic acid (i.e., dodecyl benzene sulfonic acid [DBSA]), which acts simultaneously as an emulsifier and protonating agent in the process to obtain PANI and PPy. Mild experimental conditions were adopted to achieve better structural, thermal, and electroconductive properties in the resulting nanocomposites. A comparative study of the effect of the mild polymerization conditions on the electrical conductivity with respect to the pressing pressure and the thermal stability of the nanocomposites was also carried out. This type of systematic evaluation and comparison of the thermal, electrical, and electroconductive properties of PANI/GN, PANI/GO, PPy/GN, and PPy/GO (5 wt% each) nanocomposites, synthesized through modified *in situ* EP has not been reported previously. Moreover, the electrical conductivities exhibited by nanocomposites obtained in the present study will be critically compared with those have been reported by other researchers.

EXPERIMENTAL

Materials

All chemical reagents used in this study were of analytical laboratory grade purchased from different sources and used without further purification. Graphite, aniline, DBSA, potassium permanganate ($KMnO_4$), and ammonium peroxydisulfate (APS, $(NH_4)_2S_2O_8$) were procured from Sigma-Aldrich. GN was purchased from MK Nano, Canada with a percentage purity of 99.5+ and thickness of 11–15 nm. Pyrrole (98%) was bought from Alfa Aesar and ferric chloride hexahydrate ($FeCl_{3.6}H_2O$) was purchased from Junsei Chemical, Japan. Hydrochloric acid (36.46, HCl), hydrogen peroxide (34.01, H_2O_2), sulfuric acid (98% H_2SO_4), and acetone were purchased from Dae-Jung Chemicals, South Korea.

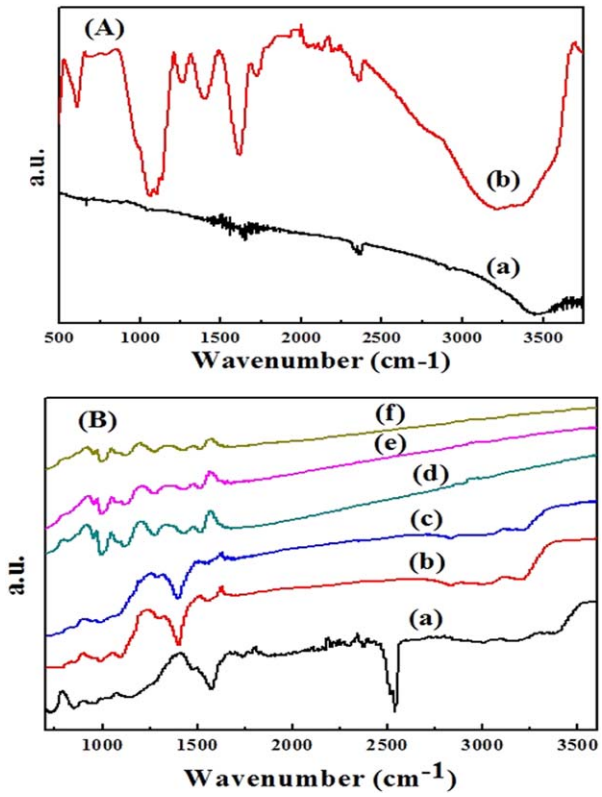


FIG. 1. (A) ATR-FTIR spectra of (a) GN and (b) GO and (B) (a) PANI, (b) PANI-GO (5 wt%), (c) PANI-GN (5 wt%), (d) PPy, (e) PPy-GO (5 wt%), and (f) PPy-GN (5 wt%). [Color figure can be viewed at wileyonlinelibrary.com]

Synthesis

Synthesis of GO. GO was prepared from natural graphite powder by modifying Hummers and Offeman's method [24]. In a typical experiment, 1 g of graphite powder was added into 17.5 ml of H_2SO_4 and stirred for 2 h while slowly adding 3 g of $KMnO_4$ to maintain the temperature of the solution at $\leq$20°C under constant stirring. The resulting mixture was then stirred at 35°C for 30 min and then at 75°C for 45 min. Twenty three millilitre of H_2O was added into the solution and heated at 90°C for 30 min at which point 75 ml of H_2O and 10 ml of a 30% H_2O_2 solution were added to terminate the oxidation. The mixture was then washed with a 5% HCl aqueous solution repeatedly until the pH became neutral. Eighty millilitre of water was added into the resulting precipitate and well-sonicated to obtain GO. The brown dispersion was centrifuged at 4,000 rpm for 2 h to remove any unexfoliated GO.

Synthesis of PANI/GN and GO Nanocomposites. For the synthesis of PANI/GN and GO nanocomposites, two different solutions containing 2.32 ml of aniline, 12.24 g of DBSA, and 125 ml of xylene was prepared in a flask. In other flasks, solutions of 10 ml deionized (DI) water, 2.34 g of APS, and 5 wt% of GN and GO were simultaneously prepared under sonication for 30 min. These solutions were then added drop-wise into the already prepared aniline solutions over a period of 30 min to avoid overheating. The polymerization reaction was allowed to proceed for 24 h and then 375 ml of acetone was added to stop the reaction. Precipitation of the solutions was then performed to obtain PANI/GN and PANI/GO complexes. A dark green powder was recovered by filtration. This was washed three times with 75 ml of acetone to remove impurities such as APS, free DBSA, and unreacted aniline monomer. Finally, both of the powders were dried in a vacuum desiccator at room temperature for 48 h.

Synthesis of PPy/GN and GO Nanocomposites. Five wt% GN and GO were dispersed in 50 ml of DI water in separate flasks and sonicated for 30 min to induce exfoliation. After sonication, 1.67 g of pyrrole was added to each of the suspensions and stirred for 1 h at 300 rpm. In separate flasks, two different solutions were prepared by adding 1.74 g of DBSA and 15.5 g of $FeCl_3.6H_2O$ in 100 ml of DI water. These solutions were added into the pyrrole/GN and pyrrole/GO solutions (5 wt%) and stirred for 4 h to allow the polymerization reaction to proceed. Once the polymerization reaction was completed, the resulting black powder was collected by filtration and washed with DI water several times to remove impurities such as $FeCl_3$, free DBSA, and unreacted pyrrole. The nanocomposites were then dried at 60°C in a vacuum oven for 24 h.

Characterization

X-ray diffraction (XRD) measurements were performed using a Rigaku rotating anode X-ray diffractometer (D/MAX-2500/PC, Rigaku, Japan) with a scanning speed of 5°/min from 10° to 60°. The instrument was equipped with a Cu-Kα radiation source (λ = 0.15418 nm) at an accelerating voltage of 50 kV and a current of 100 mA. Morphologies of the samples were studied by high-resolution transmission electron microscopy (HRTEM, JEM-2100F, JEOL; Japan) and scanning electron microscopy (SEM, JEOL JSM-6330F, Japan). Thermogravimetric analysis (TGA, TA Instruments, Q500) of the polymer nanocomposites was performed at a heating rate of 20°C/min under a nitrogen environment. Fourier transform infrared (FTIR) spectroscopic measurements of nanocomposite pellets were performed using a Nicolet iS10 between the range of 3,600 and 500 cm^{-1}. Electrical conductivities of the nanocomposite pellets were measured at room temperature using a four-probe apparatus (CMT-SR2000N, Chang Min Co, Ltd, South Korea). The average value from three measurements was reported. The pellets were prepared by compressing nanocomposites into a press (Auto M-NE, H 3981, CARVER) for 2 min. These pellets had a diameter of 10 mm, a thickness of 3–4 mm, and were pressed under pressures of 2, 4, and 6 tons.

DOI 10.1002/pc

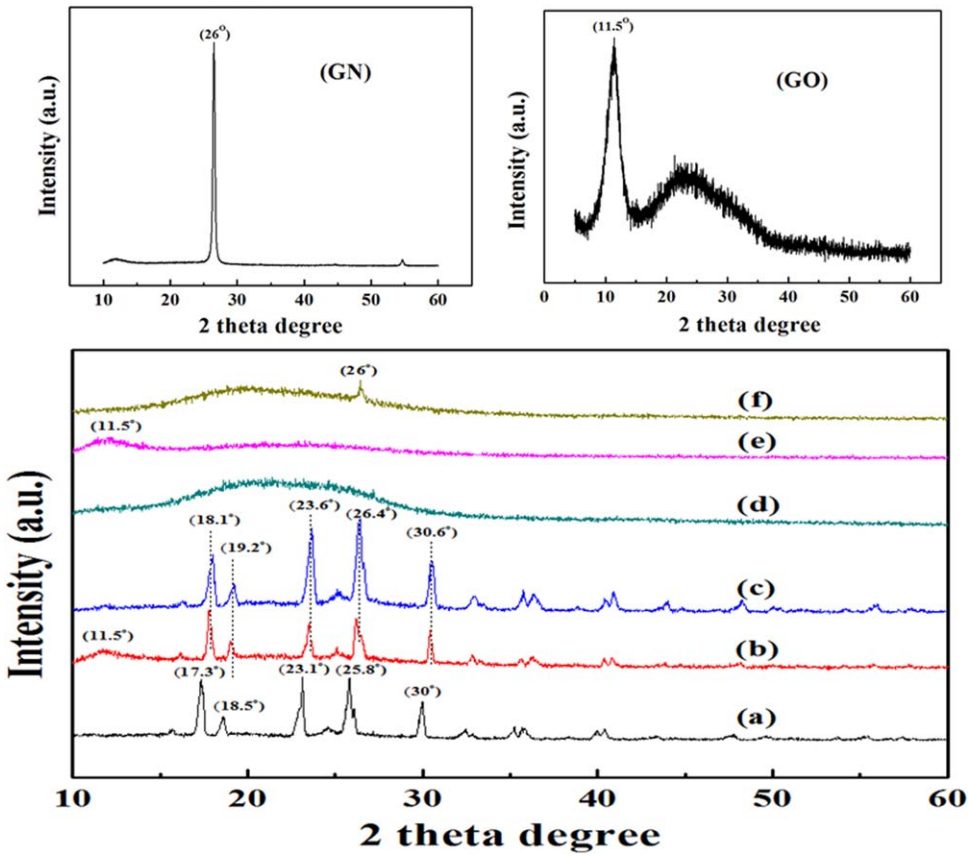


FIG. 2. XRD patterns of GN, GO, (a) PANI, (b) PANI-GO (5 wt%), (c) PANI-GN (5 wt%), (d) PPy, (e) PPy- GO (5 wt%), and (f) PPy-GN (5 wt%). [Color figure can be viewed at wileyonlinelibrary.com]

RESULTS AND DISCUSSION

Figure 1 shows the ATR-FTIR spectra of GO, GN, PANI, PPy, and their nanocomposites. In the case of GN, the band at 1,610 cm^{-1} is attributed to the C—C skeleton vibration of carbon rings in GN [25]. GO peaks at 3,213, 1,728, and 1,614 cm^{-1} are due to the OH, C═O in COOH, and vibrations of the adsorbed water molecules, which may also contain components from the skeleton vibration of unoxidized graphitic domains. The peaks at 1,059–1,410 cm^{-1} represent C—O in COH/COC functional groups [1, 3, 26]. For PANI, the absorption band at 1,580 cm^{-1} is characteristic of the imine (>C═N—) group stretching in the quinoid units. This peak is shifted to 1,404 cm^{-1} in the case of PANI/GO and to 1,390 cm^{-1} for PANI/GN nanocomposites, indicating that the carboxyl group of GO was linked to the nitrogen of the PANI backbone and to the deformation of the CO—H group, respectively, during polymerization to form crosslinked nanocomposites [3, 27, 28]. In the case of PPy, the characteristic peaks at 1,520 cm^{-1} and 1,430 cm^{-1} are related to the antisymmetric and symmetric ring stretching vibrations, respectively. The peaks at 1,120 cm^{-1} and 1,000 cm^{-1} can be attributed to the bipolaron structure of PPy, which results from DBSA doping. These peaks are also present in the nanocomposites, indicating the formation of PPy nanocomposites [29, 30].

The XRD patterns of GN, GO, PANI, PPy, and their nanocomposites are shown in Fig. 2. GN shows a diffraction peak at 26°. In the case of GO, the peak at 11.5° can be attributed to the interplanar spacing of GO sheets [5, 31–33]. For PANI, crystallization peaks appear at 17.3°, 18.5°, 23.1°, 25.8°, and 30°. Intense peaks at 18.5° and 25.8° corresponding to the (020) and (200) crystal planes, are the characteristic peaks of PANI. The other sharp peaks are due to the presence of DBSA, which acts as a surfactant and a protonating agent for the resulting PANI. Sharp peaks suggest that the resulting PANI is highly crystalline in nature [28, 34, 35]. In case of PANI nanocomposites, the results show similar peaks to those of PANI but these peaks are shifted toward right which indicates the possible interaction between PANI and layers of GN and GO in the nanocomposites. Also in case of PANI/GO nanocomposites (Fig. 2b) a peak at 11.5° can be seen that indicates the existence of GO in PANI matrix. For PPy, a broad peak in the range of 15–30° is the characteristic peak of amorphous PPy. The broadening of this peak in PPy nanocomposites clearly indicates that

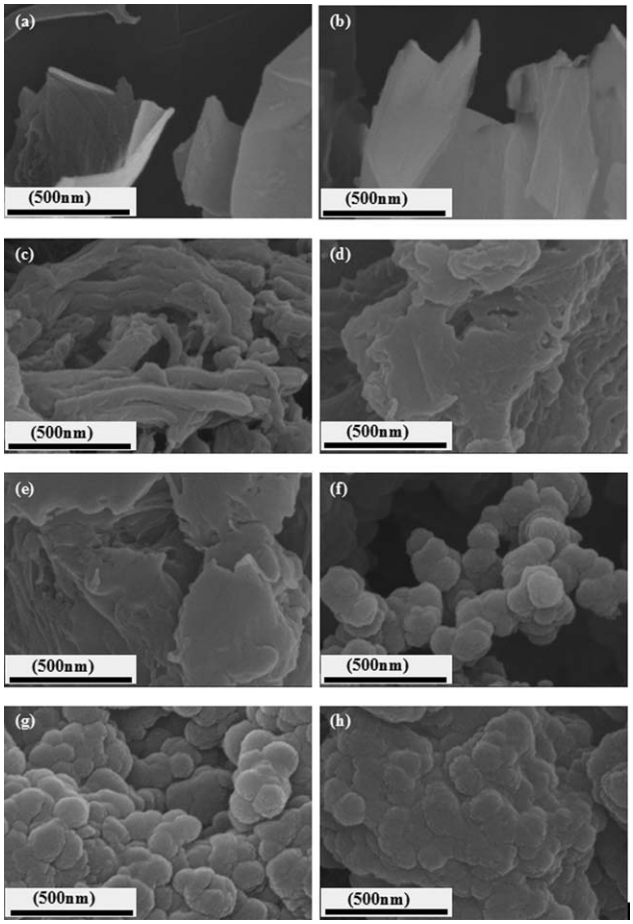


FIG. 3. FESEM images of (a) GO, (b) GN, (c) PANI, (d) PANI-GO (5 wt%), (e) PANI-GN (5 wt%), (f) PPy,(g) PPy-GO (5 wt%), and (h) PPy-GN (5 wt%).

there is an interaction between PPy and the layers of GN and GO [4, 31, 32].

Figure 3 shows the FE-SEM images of GO, GN, PANI, PPy, and their nanocomposites. It can be seen in Fig. 3a that GO has a wrinkled structure and many folded regions with a lateral size of several micrometers [36]. In the case of GN nanosheets (Fig. 3b), a clean and uniform surface can be observed [37, 38]. Fiber-like structures can be observed in the case of PANI, whereas PPy shows a spherical particle-like structure with an average particle size up to 300 nm. The morphologies of PANI and PPy nanocomposites with GN and GO are different from those of PANI and PPy. This is due to the presence of GN and GO during the polymerization of the polymers, which results in the sheet-like structure of the final nanocomposites due to the fact that GN and GO serve as templates during the formation of nanocomposites [39, 40].

Figure 4 shows the HR-TEM images of GO, GN, PANI, PPy, and their nanocomposites. GN has a very thin, transparent, and uniform surface whereas GO shows a wrinkled structure. This was also confirmed by the FESEM results discussed earlier. On the addition of GN and GO into the matrix of PANI and PPy, the polymer morphologies changed from tube-like (in the case of PANI) and spherical (in the case of PPy) particles into sheet-like structures; this was caused by the same reason that was discussed in the FE-SEM results: the polymerization reaction is carried out on the GN and GO sheets to form a sheet-like structure. It is important to note that the GN and GO sheets are uniformly distributed in the PANI and PPy matrices and that no agglomerates can be seen; this is crucial for enhancing the thermal and electrical properties of the nanocomposites.

The TGA results for GO, GN, PANI, PPy, and their nanocomposites are shown in Fig. 5. It can be seen that GN showed high thermal stability; a total weight loss of only 14% occurred at 800°C. Alternatively, in the case of GO, a total weight loss of 53% is registered; this is due to the evaporation of the moisture present in the sample and to the weight loss between 200 and 300°C (about 23%), which is due to the removal of oxygen-containing groups like carboxyl (—COOH) and hydroxyl (—OH) groups. In the case of PANI, the notable weight loss between 200 and 600°C can be assigned to the thermal degradation of bound BDSA in the PANI matrix; there was a total weight loss of 75% at 800°C in the case of PANI. In case of PANI nanocomposites with GN and GO the thermal stability is almost similar to that of pure

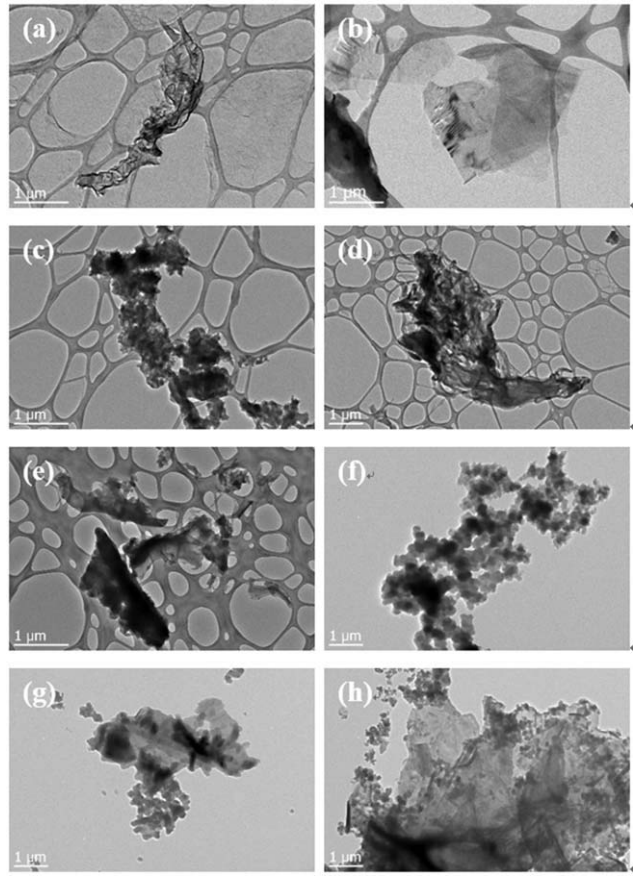


FIG. 4. HRTEM images of (a) GO, (b) GN, (c) PANI, (d) PANI-GO (5 wt%), (e) PANI-GN (5 wt%), (f) PPy,(g) PPy-GO (5 wt%), and (h) PPy-GN (5 wt%).

 DOI 10.1002/pc

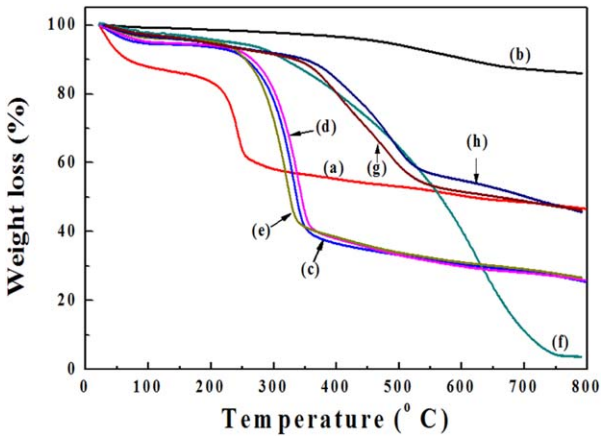


FIG. 5. TGA analysis of (a) GO, (b) GN, (c) PANI, (d) PANI-GO (5 wt%), (e) PANI-GN (5 wt%), (f) PPy,(g) PPy-GO (5 wt%), and (h) PPy-GN (5 wt%). [Color figure can be viewed at wileyonlinelibrary.com]

PANI, a total weight loss of 73% was registered for PANI/GN (5 wt%) and a total weight loss of 74% was observed for the case of PANI/GO nanocomposites. For PPy, the degradation starts around 280°C, and a weight loss of almost 97% can be seen at 800°C, which means that PPy is highly unstable at high temperatures; however, by adding GN and GO into the PPy matrix, the thermal stability of the nanocomposites increased dramatically: as the starting degradation temperatures increased from 280°C in case of PPy to 345°C in case of PPy nanocomposites and a weight loss of ~46% was registered for the nanocomposites at 800°C. It can be seen from the TGA curves that PPy/GO nanocomposites showed sharp decrease in weight as compared to PPy/GN nanocomposites between the ranges of 345°C to 720°C. This is due to the fact that the addition of GN sheets in the polymer restricts the mobility and thermal vibrations of PPy chains at the GN-PPy interface, eventually delaying the degradation of PPy chains [41, 42].

In our previous studies [9, 17], we prepared PANI/GO and PPy/GN nanocomposites with different GO/GN loadings (1, 2, and 5 wt%). We demonstrated that the electrical conductivities of the nanocomposite pellets increased sharply with increasing GO/GN content and applied pressure. Nanocomposites with 5 wt% GO/GN loadings showed the highest electrical conductivity. We have also discussed how the electrical properties of nanocomposites depend on a variety of factors including the morphology of the nanocomposites, particle size, structure, and synthesis method. Based on these previous findings, we prepared nanocomposites of PANI and PPy with 5 wt% GO and GN in this study. Pellets were prepared at different pressing pressures ranging from 2 to 6 tons to systematically study the effect of the pressing pressure on the electrical properties of the conductive polymer/GO/GN nanocomposites.

The electrical conductivities of the nanocomposites were measured with a four-probe method, as shown in Fig. 6. It can be seen that the electrical conductivities of PANI, PPy, and their nanocomposites increased as the pressing pressure increased. This increase is relatively sharp up to 4 tons of pressure and then becomes almost linear for the PANI/GN and PPy/GN nanocomposites; this demonstrates that a considerable amount of the voids are removed from the GN nanocomposites at 4 tons. In the case of PANI, the electrical conductivity increases from 41.06 S/m (at 2 tons) to 218.9 S/m (at 6 tons). These values are quite high when compared to previously reported literature values at room temperature. For PPy, the initially measured conductivity was 19.71 S/m; this was increased to 77.24 S/m at 6 tons. PPy/GO showed higher electrical conductivity than PANI/GO, which could be due to the enhanced interaction between the GO and PPy layers [43]. PPy/GN nanocomposites showed the highest electrical conductivities at a variety of pressures (at 2 tons the conductivity was 494.7 S/m and at 6 tons the conductivity was 643.5 S/m), whereas PANI/GN nanocomposites showed lower conductivities of 469.2 S/m and 601.4 S/m at 2 and 6 tons, respectively. The fact that PPy nanocomposites show superior electrical conductivities at different pressing pressures demonstrates how GO and GN have better interactions with PPy compared to PANI; this can be attributed to the high aspect ratio and large surface area of GO and GN in the PPy matrix.

Recent studies have reported the electrical properties of various conductive polymers such as PANI, PPy, and their nanocomposites with GO and GN. Table 1 summarizes some of the recently reported electrical conductivities of PANI, PPy, and their nanocomposites with different amounts of GO and GN. Stejskal et al. [22] prepared PANI and PPy in the presence of different surfactants via oxidative polymerization. An electrical conductivity of 4.9 S/m was reported for PPy at room temperature without using any surfactants during

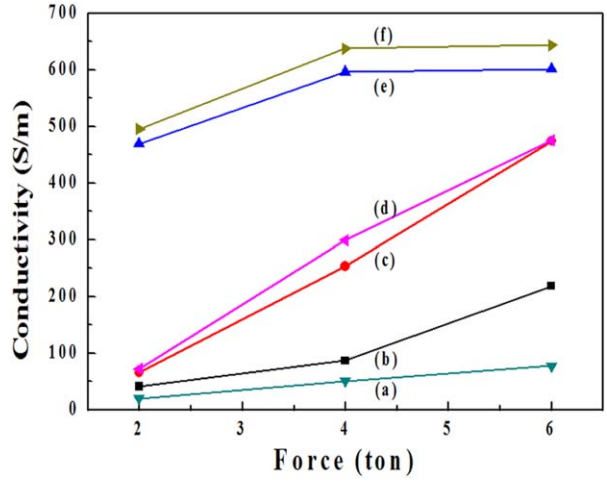


FIG. 6. Electrical conductivities of (a) PPy, (b) PANI, (c) PANI-GO (5 wt%), (d) PPy-GO (5 wt%), (e) PANI-G (5 wt%), and (f) PPy-G (5 wt%). [Color figure can be viewed at wileyonlinelibrary.com]

TABLE 1. Reported electrical conductivities of conductive polymers and their nanocomposites with GO and G by various researchers at different conditions.

Report	Sample name	Pressing pressure (MPa)	Measurement temperature (°C)	GO/G wt%	Conductivity (S/m)
Stejskal et al. [22]	PPy	—	20	—	4.9
	PPy-DBSA				990
Tabaciarova et al. [44]	PPy-Cl	30	20		420
Manival et al. [45]	PPy	—	25	—	18
Manival et al. [45]	PPy-GO	—	25	5	34.6
Zhong et al. [46]	PPy-GO	—	25	3	11
Jie Xu et al. [47]	PPy-RGO	—	25	—	120
Ramasamy et al. [48]	PPy-GN		25	90	26
				50	14
				25	0.4
Xiao et al. [49]	PANI	700	—	—	406
Oral [50]	PANI	—	—	—	59
Lin et al. [51]	P-CGO		25	10	49
	P-CGO			5	20
	P-CGO			100	18
	P-GO			10	1.23
Yang et al. [52]	PANI- GO	—	25	—	0.058
Boeva et al. [53]	PANI-GN	—	25	—	37
Zhang et al. [54]	PANI-GN	—	—	10	168.7
				50	22.8
				80	143
Our study	PANI/GO	6	25	5	473.84
	PANI/GN				601.4
	PPy/GO				475.67
	PPy/GN				643.5

P-CGO (PANI-CTAB intercalated GO), P-GO (PANI-GO).

polymerization. Alternatively, for PPy-DBSA, an electrical conductivity of 990 S/m was reported. It can be concluded from the above report that the presence of a surfactant during the polymerization of conductive polymers can have a significant influence on the final conductive properties of the resulting polymers. Tabaciarova et al. [44] also reported the preparation and electrical conductivity of PPy made via oxidative polymerization with four different oxidants. For PPy-Cl, the reported conductivity was 420 S/m. Manivel et al. [45] synthesized PPy/GO nanocomposites via *in situ* polymerization with different amounts of GO (1–5 wt%). At room temperature, the conductivity of pure PPy with an HCl medium was reported to be 18 S/m; in the case of PPy/GO (5 wt%) nanocomposites, the reported conductivity was 34.6 S/m. The reason for the improvement in conductivity on the addition of GO into the polymer matrix is related to the high surface area of GO, which serves as a bridge to conduct electric current. The highest electrical conductivity reported by Zhong et al. [46] for PPy/GO (3 wt%) was 11 S/m. Jie et al. [47] reported the synthesis of PPy/RGO made via chemical polymerization. They obtained an electrical conductivity of 120 S/m. Ramasamy et al. [48] synthesized PPy-grafted graphene sheets (GS) via chemical oxidative polymerization with different weight ratios of GS:PPy (90:10, 50:50, and 25:75) and measured electrical conductivities of 26, 14, and 0.4 S/m, respectively. Xiao et al. [49] and Oral et al. [50] reported the polymerization of PANI via chemical oxidative polymerization. They determined that the conductivity of PANI was 406 and 59 S/m, respectively. Similarly, there are a number of researchers who have synthesized PANI nanocomposites and reported conductivity values; some of these are summarized in Table 1.

Lin et al. [51] prepared PANI/GO nanocomposites via *in situ* polymerization in the presence of cetyltrimethylammonium bromide (CTAB). The reported conductivity values for PANI/CTAB intercalated GO (CGO) nanocomposites with CGO (10, 5, and 100 wt%) were 49, 20, and 18 S/m, respectively. The conductivity of PANI/GO was determined to be 1.23 S/m. Alternatively; Yang et al. [52] prepared PANI/GO nanocomposites by directly adding a GO aqueous solution into the emeraldine base form of PANI. To improve the conductivity, PANI/GO was redoped with 1 M HCl as a dopant, and the conductivity obtained at room temperature was 0.058 S/m. Beova et al. [53] and Zhang et al. [54] reported the synthesis of PANI/GN nanocomposites via the *in situ* polymerization of aniline. The electrical conductivity reported by Beova et al. was 37 S/m, whereas Zhang et al. reported the electrical conductivity for PANI/GN (10, 50, and 100 wt%) to be 168.7, 22.8, and 143 S/m, respectively. All of these studies indicate that there are numerous factors that influence the final electrical properties of conductive polymers and their nanocomposites. These factors include the type of dopant, method of polymerization, morphology of the

 DOI 10.1002/pc

conductive polymers and their nanocomposites, and the chain structure of the conductive polymers. Our study demonstrates that by using DBSA as a surfactant and a dopant during the *in situ* EP of conductive polymers, we can obtain conductive polymers with superior morphology and enhanced conductivity. Additionally, with the addition of various conductive fillers (e.g., GO and GN), the electrical conductivities can be further enhanced up to 601.4 and 643.5 S/m for PANI/GN and PPy/GN nanocomposites, respectively, and up to 473.84 and 475.67 in the case of PANI/GO and PPy/GO nanocomposites, respectively (at room temperature and a pressing pressure of 6 tons). These values are very high compared to the values reported in the literature. This type of systematic study, looking into the electrical conductivities of different conductive polymers with GO and GN at different pressing pressures, has rarely been reported.

CONCLUSIONS

In this study, we reported the synthesis and characterization of two different conductive polymers (PANI and PPy) and their nanocomposites with GO and GN (5 wt%). These polymers were modified via *in situ* EP using DBSA as both a surfactant and a doping agent. AT-FTIR results showed the successful interaction between the polymer chains and GO/GN. The XRD peaks for PANI and its nanocomposites were very sharp, indicating that they were crystalline in nature, whereas the broadened PPy peak in the case of PPy nanocomposites indicated the interaction between PPy and the GO/GN layers. FESEM results indicated that the resulting nanocomposites of both conductive polymers had sheet-like morphologies due to the presence of GO and GN during polymerization. Additionally, TEM results confirmed that PANI and PPy were well-distributed on the surface of GO and GN. TGA results clearly indicated that the thermal properties were enhanced on the addition of GO and GN in the conductive polymer matrices. All of the nanocomposites demonstrated higher values of electrical conductivity at room temperature with 5 wt% of GO and GN as doping agents. PPy nanocomposites with GO and GN showed the highest electrical conductivities (475.67 and 643.5 S/m, respectively) due to the improved interaction of PPy chains with GO and GN, as compared to PANI. This work provides an effective and reproducible method to fabricate conductive polymers (and their nanocomposites) that possess superior and desirable structural and electrical properties for various semiconductor devices.

REFERENCES

1. G. Venugopal, K. Krishnamoorthy, R. Mohan, and S.J. Kim, *Mater. Chem. Phys.*, **132**, 29 (2012).
2. X. Lu, H. Dou, S. Yang, L. Hao, L. Zhang, L. Shen, F. Zhang, and X. Zhang, *Electrochim. Acta*, **56**, 9224 (2011).
3. H. Wang, Q. Hao, X. Yang, L. Lu, and X. Wang, *Electrochem. Commun.*, **11**, 1158 (2009).
4. X. Yan, X. Zhang, H. Liu, Y. Liu, J. Ding, Y. Liu, Q. Cai, and J. Zhang, *Synth. Met.*, **196**, 1 (2014).
5. Y.F. Huang and C.W. Lin, *Polymer*, **53**, 2574 (2012).
6. X. Lua, W. Zhanga, C. Wanga, T.C. Wenb, and Y. We, *Prog. Polym. Sci.*, **36**, 671 (2011).
7. X. Li, Q. Zhong, X. Zhang, T. Li, and J. Huang, *Thin Solid Films*, **584**, 348 (2015).
8. P. He, B. Huang, L. Liu, Q. Huang, and T. Chen, *Polym. Compos.*, **37**, 1515 (2014).
9. S.M. Imran, G.N. Shao, M.S. Haider, N. Abbas, M. Hussain, and H.T. Kim, *J. Appl. Polym. Sci.*, **132**, (2015). n/a-n/a,
10. J.C. Chiang and A.G. MacDiarmid, *Synth. Met.*, **13**, 193 (1986).
11. J.E. Österholm, Y. Cao, F. Klavetter, and P. Smith, *Polymer*, **35**, 2902 (1994).
12. D. Zhang, *Polym. Test.*, **26**, 9 (2007).
13. Y. Xia, J.M. Wiesinger, A.G. MacDiarmid, and A.J. Epstein, *Chem. Mater.*, **7**, 443 (1995).
14. M. Amaike and H. Yamamoto, *Polym. J.*, **38**, 703 (2006).
15. S. Košina, S. Balúch, J. Annus, M. Omastová, and J. Krištín, *J. Mater. Sci.*, **29**, 3403 (1994).
16. T. Kuilla, S. Bhadra, D. Yao, N.H. Kim, S. Bose, and J.H. Lee, *Prog. Polym. Sci.*, **35**, 1350 (2010).
17. S.M. Imran, Y. Kim, G. Shao, M. Hussain, Y. Choa, and H. Kim, *J. Mater. Sci.*, **49**, 1328 (2014).
18. P.J. Kinlen, J. Liu, Y. Ding, C.R. Graham, and E.E. Remsen, *Macromolecules*, **31**, 1735 (1998).
19. S. Palaniappan, *Polym. Adv. Technol.*, **13**, 54 (2002).
20. H. Xia and Q. Wang, *J. Nanopart. Res.*, **3**, 399 (2001).
21. N.V. Blinova, J. Stejskal, M. Trchová, J. Prokeš, and M. Omastová, *Eur. Polym. J.*, **43**, 2331 (2007).
22. J. Stejskal, M. Omastová, S. Fedorova, J. Prokeš, and M. Trchová, *Polymer*, **44**, 1353 (2003).
23. D. Ichinohe, T. Aral, and H. Kise, *Synth. Met.*, **84**, 75 (1997).
24. W.S. Hummers and R.E. Offeman, *J. Am. Chem. Soc.*, **80**, 1339 (1958).
25. F. Xiao, S. Yang, Z. Zhang, H. Liu, J. Xiao, L. Wan, J. Luo, S. Wang, and Y. Liu, *Sci. Rep.*, **5**, 9359 (2015).
26. L. Wang, Y. Ye, X. Lu, Z. Wen, Z. Li, H. Hou, and Y. Song, *Sci. Rep.*, **3**, 3568 (2013).
27. H. Liu, W. Zhang, H. Song, X. Chen, J. Zhou, and Z. Ma, *Electrochim. Acta*, **146**, 511 (2014).
28. Y. Zhao, G.S. Tang, Z.Z. Yu, and J.S. Qi, *Carbon*, **50**, 3064 (2012).
29. H.C. Kang and K.E. Geckeler, *Polymer*, **41**, 6931 (2000).
30. M. Kotal, S.K. Srivastava, and B. Paramanik, *J. Phys. Chem. C*, **115**, 1496 (2011).
31. X. Wang, C. Yang, H. Li, and P. Liu, *Electrochim. Acta*, **111**, 729 (2013).
32. W.D. Lin, H.M. Chang, and R.J. Wu, *Sens. Actuators B*, **181**, 326 (2013).
33. Q. Huang, D. Zeng, S. Tian, and C. Xie, *Mater. Lett.*, **83**, 76 (2012).

34. N.A. Kumar, H.J. Choi, Y.R. Shin, D.W. Chang, L. Dai, and J.B. Baek, *ACS Nano*, **6**, 1715 (2012).
35. D. Han, Y. Chu, L. Yang, Y. Liu, and Z. Lv, *Colloids Surf. A*, **259**, 179 (2005).
36. Y.F. Huang and C.W. Lin, *Polymer*, **53**, 1079 (2012).
37. C. Xu, J. Sun, and L. Gao, *J. Mater. Chem.*, **21**, 11253 (2011).
38. Y. Liu, H. Wang, J. Zhou, L. Bian, E. Zhu, J. Hai, J. Tang, and W. Tang, *Electrochim. Acta*, **112**, 44 (2013).
39. L. Yu, Y. Zhang, W. Tong, J. Shang, F. Lv, P.K. Chu, and W. Guo, *Compos. Part A*, **43**, 2039 (2012).
40. F.H. Hsu and T.M. Wu, *Synth. Met.*, **162**, 682 (2012).
41. S. Sahoo, G. Karthikeyan, G.C. Nayak, and C.K. Das, *Synth. Met.*, **161**, 1713 (2011).
42. K. Lozano and E.V. Barrera, *J. Appl. Polym. Sci.*, **79**, 125 (2001).
43. S. Bose, T. Kuila, M.E. Uddin, N.H. Kim, A.K.T. Lau, and J.H. Lee, *Polymer*, **51**, 5921 (2010).
44. J. Tabačiarová, M. Mičušík, P. Fedorko, and M. Omastová, *Polym. Degrad. Stab.*, **120**, 392 (2015).
45. P. Manivel, S. Kanagaraj, A. Balamurugan, N. Ponpandian, D. Mangalaraj, and C. Viswanathan, *J. Appl. Polym. Sci.*, **131** (2014).
46. J. Zhong, S. Gao, G. Xue, and B. Wang, *Macromolecules*, **48**, 1592 (2015).
47. J. Xu, D. Wang, Y. Yuan, W. Wei, L. Duan, L. Wang, H. Bao, and W. Xu, *Org. Electron*, **24**, 153 (2015).
48. M.S. Ramasamy, S.S. Mahapatra, and J.W. Cho, *J. Colloid Interface Sci.*, **455**, 63 (2015).
49. H.M. Xiao, W.D. Zhang, L. Na, G.W. Huang, Y. Liu, and S.Y. Fu, *J. Polym. Sci. Part A-1 Polym. Chem.*, **53**, 1575 (2015).
50. I. Oral, *J. Appl. Polym. Sci.*, **132** (2015).
51. S.J. Lin, H.J. Sun, T.J. Peng, and L.H. Jiang, *High Perform. Polym.*, **26**, 790 (2014).
52. N. Yang, J. Zhai, M. Wan, D. Wang, and L. Jiang, *Synth. Met.*, **160**, 1617 (2010).
53. Z.A. Boeva, K.A. Milakin, M. Pesonen, A.N. Ozerin, V.G. Sergeyev, and T. Lindfors, *RSC Adv.*, **4**, 46340 (2014).
54. K. Zhang, L.L. Zhang, X.S. Zhao, and J. Wu, *Chem. Mater.*, **22**, 1392 (2010).

 DOI 10.1002/pc